

Report

TexAQS-II Dual-Doppler Wind Data

Grant Activity No. 582-5-64593-FY07-20

Analysis of TexAQS II Meteorological Data

A report to the Texas Commission on Environmental Quality

Andrew P. McNeel

John W. Nielsen-Gammon

Department of Atmospheric Sciences

Texas A&M University

College Station, Texas

December 7, 2007

Contact information:

John W. Nielsen-Gammon

Dept. of Atmospheric Sciences

Texas A&M University

3150 TAMUS

College Station, TX 77843-3150

979-862-2248

n-g@tamu.edu

1. Overview

Data collected during TexAQS-II by the Shared Mobile Atmospheric Research and Teaching (SMART) Radar “SR1” has been coupled with radar data from the National Weather Service’s weather surveillance Doppler radar “KHGX” to produce dual-Doppler wind fields for the Houston area during the campaign. This report documents the production of these wind fields and the investigation into the feasibility and effectiveness of assimilating these derived wind fields into mesoscale models to improve simulation accuracy.

2. Radar Data

The SMART Radars, a joint facility of the National Severe Storms Laboratory, Texas A&M University, Texas Tech University, and The University of Oklahoma, are 5 cm C-band Doppler radars that have been mounted to flatbed trucks for easy mobility. During the TexAQS-II study, two SMART Radars were deployed - one to the Houston area, and one to the Dallas/Fort Worth area - and strategically positioned in such a way that dual-Doppler synthesis could eventually be possible utilizing the nearby National Weather Service WSR-88D radars (KHGX and KFWD, respectively) and where obstructions and obstacles would be at a minimum.

The SMART Radar “SR1” was positioned at La Porte Municipal Airport, approximately 22 km north of the KHGX National Weather Service radar. Here, it was in operation from 11 July, 2005 to 21 September, 2005. During this time, it gathered approximately 1,624 hours (186 GB) of data. SR1’s boundary surveillance scans yielded data roughly every three minutes, except during convective events. During convective events, the radar ran in precipitation mode, and it provided boundary surveillance scans approximately every ten minutes. During the time period of the study, SR1 experienced approximately 6% down time due to technical issues, mechanical issues, and re-fueling.

The KHGX National Weather Service radar is a Weather Surveillance Radar – 1988 Doppler (WSR-88D) S-band (10 cm) Doppler radar operated by the National Weather Service Office in League City. Unless convergence and/or convection are present in the area of the radar, KHGX completes scans approximately every ten minutes. If convergence is present, scans are completed every six minutes, and if convection is present, scans are completed every five minutes. During the period that SR1 was present and gathering data in La Porte, KHGX experienced less than 1% down time. Figure 1 shows the locations of the SR1 and KHGX radars during the data-collection period.

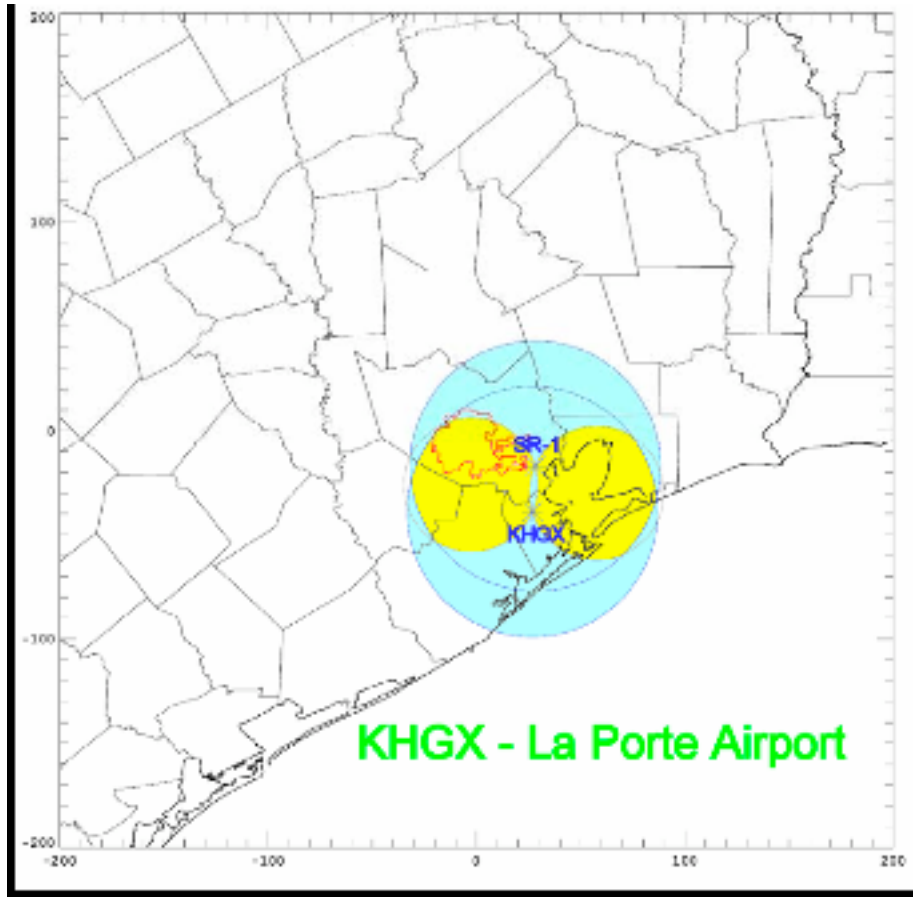


Figure 1: Configuration of the SR1 and KHGX radars during the data-collection period (11 July - 21 September, 2005), with single-Doppler (blue) and dual-Doppler (yellow) lobes (from Carey et al. 2005).

3. Methodology

Radars transmit radiation at a fixed wavelength in an effort to receive a return signal from the transmitted radiation reflecting off of an object in the air. Doppler radars are capable of gathering information about the velocity of a moving object by measuring the Doppler shift in the wavelength of the radiation being reflected back to the radar by that object.

However, radars are thus only capable of detecting one component of the velocity of the object, that being the radial velocity, or, the component moving towards or away from the radar parallel to the radar beam. Therefore, if two radars could be employed to gather information about the velocity of an object, they would be able to detect two different components of the object's actual velocity, thus making it possible to derive the actual velocity of the object. Such is the concept of dual-Doppler analysis of velocity.

Boundary layer winds are determined based on "clear-air" (non-precipitation) returns. These clear-air returns are a result of the detection of atmospheric tracers on the order of 1-10 mm as they are transported by the wind, thus providing an indication of boundary layer wind speed and direction. Doppler radars are very sensitive to small tracer objects such as these in the atmosphere. Insects are the most commonly tracer objects responsible for clear-air returns. Although insects fly with a velocity themselves, their flight patterns are random, and therefore do not significantly contaminate the boundary layer wind values derived from their radar signature, as determined by Wilson et al. (1994). Birds can also be responsible for clear-air returns, and most of the time they tend not to contaminate velocity data. However, mass bird migrations can cause a significant bias in velocity (Gauthreaux et al. 1998). Clear-air returns can also occur as a result of turbulent variations in the refractive index of the atmosphere on a scale on the order of the radar's wavelength, causing a reflection of the radar signal.

The SMART Radar is capable of these detections at a range of 45-75 km horizontally and 0-3 km vertically. The WSR-88D is capable of these returns at a range of approximately

50-100 km horizontally and 0-3 km vertically. Detection of winds above the boundary layer by the SMART radar or WSR-88D is generally poor in the absence of precipitation.

4. Data Synthesis

Data from SRI in its raw IRIS format and data from KHGX in its raw Level II format were translated from radar coordinates (elevation, azimuth, and range) using NCAR's XLTRSII data translator. XLTRSII is a binary program that converts raw radar data into NCAR sweep format, also known as universal format (UF). In this format, Radar data can then be gridded using NCAR's program REORDER (see Oye and Case, 1995).

Beam pointing angles in the SR1 data was corrected for any errors in heading that may have been incurred due to positioning the radar. The correction was 2.3 degrees, and this was done with a FORTRAN program developed by Larry Carey that also cleaned up ground clutter from the data. Ground clutter was defined as any radar sample with a radial velocity of $-0.25 - 0.25 \text{ ms}^{-1}$ or with a spectral width less than 0.7 ms^{-1} . Any samples meeting one or both of these criteria were removed by the program. These criteria for ground clutter represent an attempt at balance between excluding ground features and keeping most of the valid clear-air and precipitation returns. WSR-88D Level II data were already corrected for ground clutter by the National Weather Service using a clutter mitigation scheme.

SR1 and KHGX data in UF format were converted from polar radar coordinates to Cartesian coordinates using NCAR's REORDER program. Grid spacing was set at 1 km in the horizontal and 200 m in the vertical, with a maximum height of 2 km. In interpolating to each grid point, a Cressman weighting scheme was employed, which gives more weight to radar values closer to the actual grid point. This weighting scheme is a function of the radii of influence and the distance of the radar gate to the grid point. The radii of influence were varied in an effort to produce a plot that exhibited sufficiently representative boundary layer winds in the region while still covering an acceptably large portion of the region. Horizontal radii of influence were varied from 1-3 km, and the vertical radius of influence was varied from 100-400 m.

Once REORDER had converted the UF format radar data from both radars into Cartesian coordinates from polar coordinates, dual-Doppler synthesis was done using the NCAR program CEDRIC (Custom Editing and Display of Reduced Information in Cartesian space). In this process, scans from both radars were matched to within every three minutes. This resulted in grids at approximately ten-minute intervals. An Interactive Data Language (IDL) script was then employed to produce plots of these grids, as shown in Figure 2.

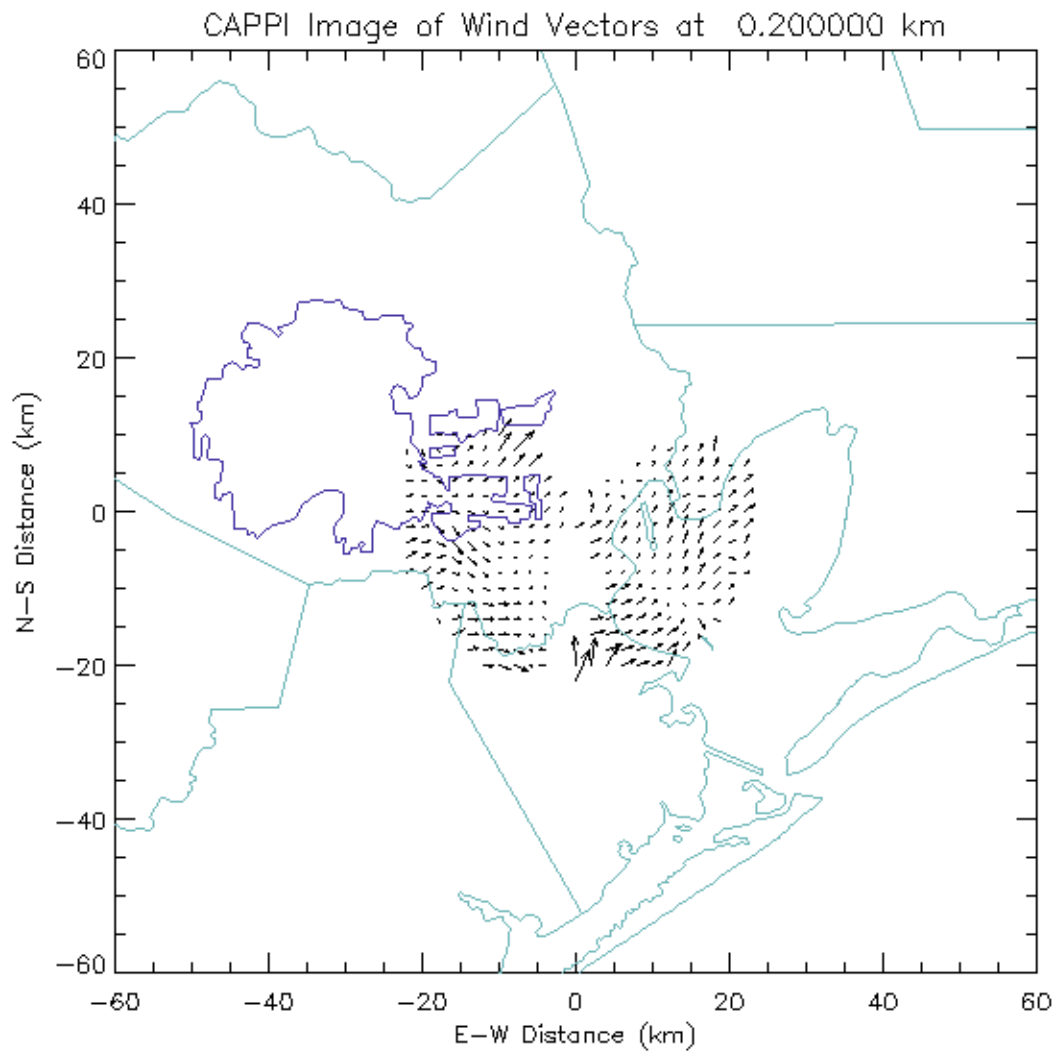


Figure 2: Wind vectors derived from dual-Doppler analysis of radar data from the SR1 SMART Radar and the KHGX National Weather Service radar, 1511 UTC 12 August 2005.

5. Results

One of the goals of this study was to determine an ideal set of parameters for the minimum beam-crossing angle and the horizontal and vertical radii of influence so as to achieve a satisfactory balance between the quality of the wind data and the area covered. The acceptability of the balance between these two qualities is an important factor to consider if the data is to be assimilated into mesoscale models.

The dual-Doppler beam-crossing angle, β , is defined as the angle between the lines passing through a given point and each of the two radar locations. The accuracy of the retrieved velocity components depends on β as follows:

$$\frac{\sigma_u^2 + \sigma_v^2}{\sigma_1^2 + \sigma_2^2} = \csc^2 \beta \quad (5.1)$$

where σ_u and σ_v are the error variances of the u and v components of the wind, respectively, and σ_1 and σ_2 are the error variances of the radial velocities of the two radars. Hence, as the beam-crossing angle is increased, error variances in the u and v components of the wind are decreased. A beam-crossing angle of 90° is ideal. However, as the beam crossing angle increases, the area of the analysis domain also decreases.

The area of the analysis domain, A_1 , is given by:

$$A_1(\beta_o) = 2(d \csc \beta_o)^2(\pi - 2\beta_o + 2 \sin 2\beta_o) \quad (5.2)$$

where β_o is the minimum allowed beam crossing angle.

A minimum beam-crossing angle of 30° was selected (i.e., all beam-crossing angles between 30° and 90°) to yield an adequate size for the analysis domain while maintaining satisfactory error variances.

Values for horizontal and vertical radii of influence were varied in order to achieve satisfactory data resolution while maintaining a representative depiction of boundary-layer winds across the region. Smaller values for horizontal radii of influence improve data resolution, but subjects the field to noise, while larger values for horizontal radii of influence reduces the resolution of the data, but improves how well the derived field represents the actual wind pattern across the region (see Figure 3-5). Care is necessary in choosing the vertical radius of influence as well due to the risk of sampling outside of the boundary layer, as well as for the reasons listed above for horizontal radii of influence. In varying the values for the horizontal and vertical radii of influence, it was determined that 3 km horizontal radii of influence in both the x and y direction and a 200 m vertical radius of influence provided a satisfactory balance between data resolution and representativeness.

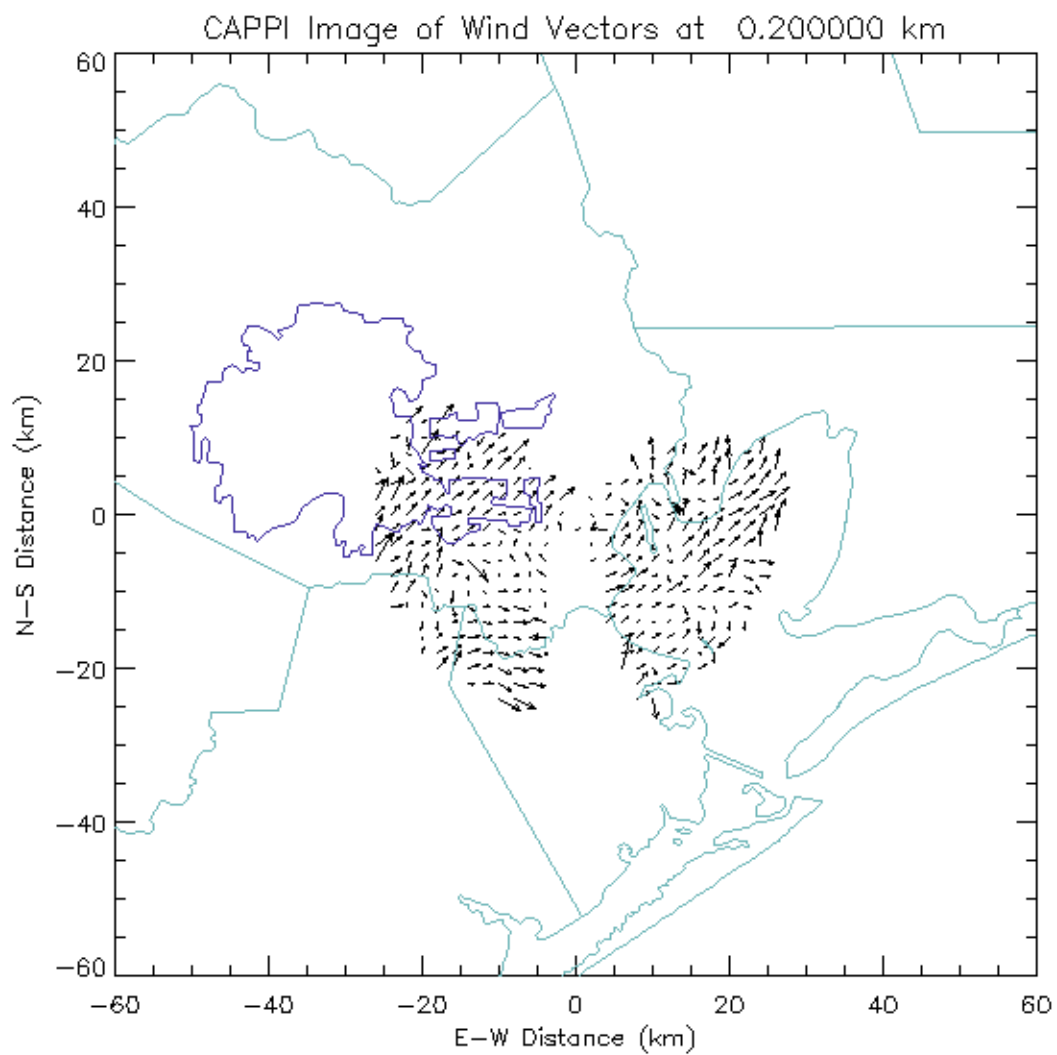


Figure 3: Dual-Doppler derived wind field at a height of 200 m using 1 km horizontal radii of influence and 200 m vertical radius of influence, 1536Z 10 August 2005.

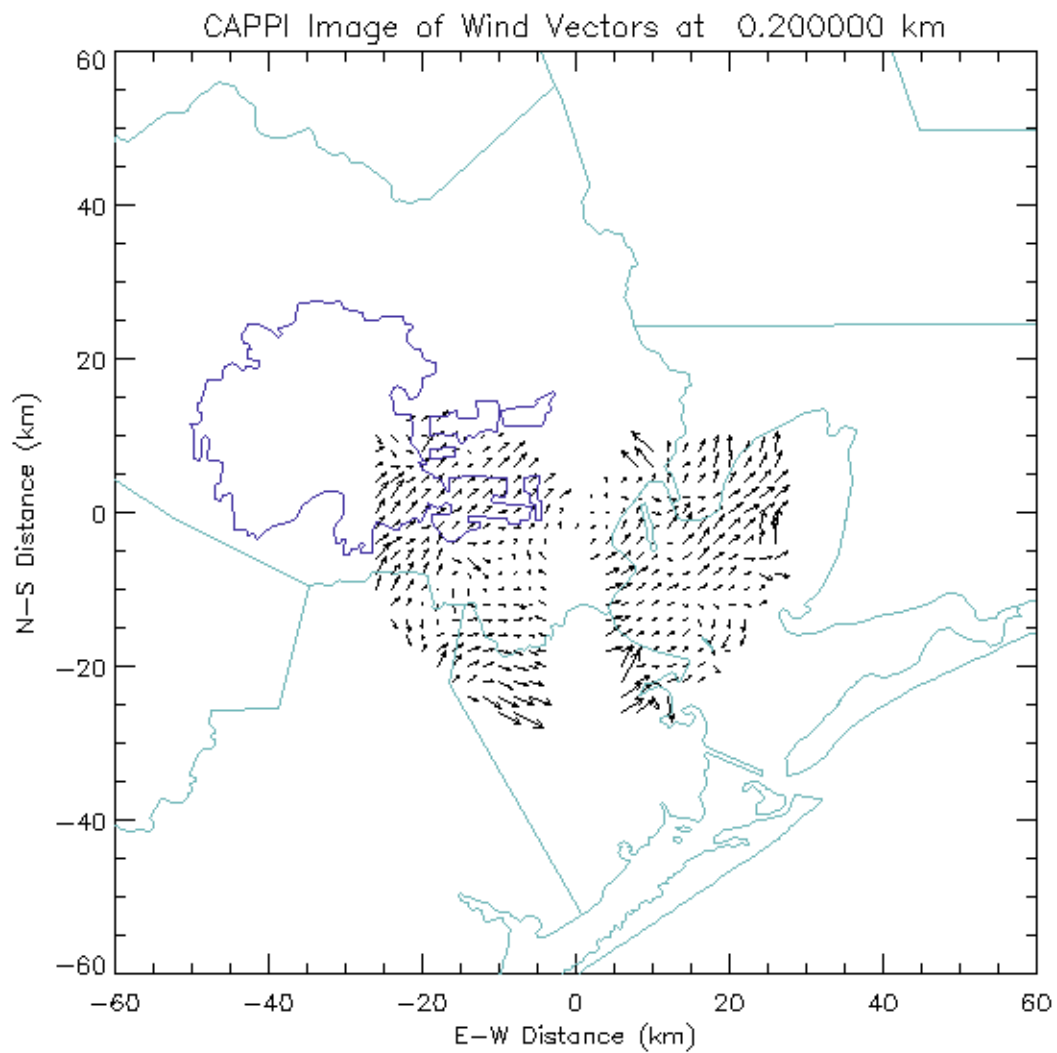


Figure 4: Dual-Doppler derived wind field at a height of 200 m using 2 km horizontal radii of influence and 200 m vertical radius of influence, 1536Z 10 August 2005.

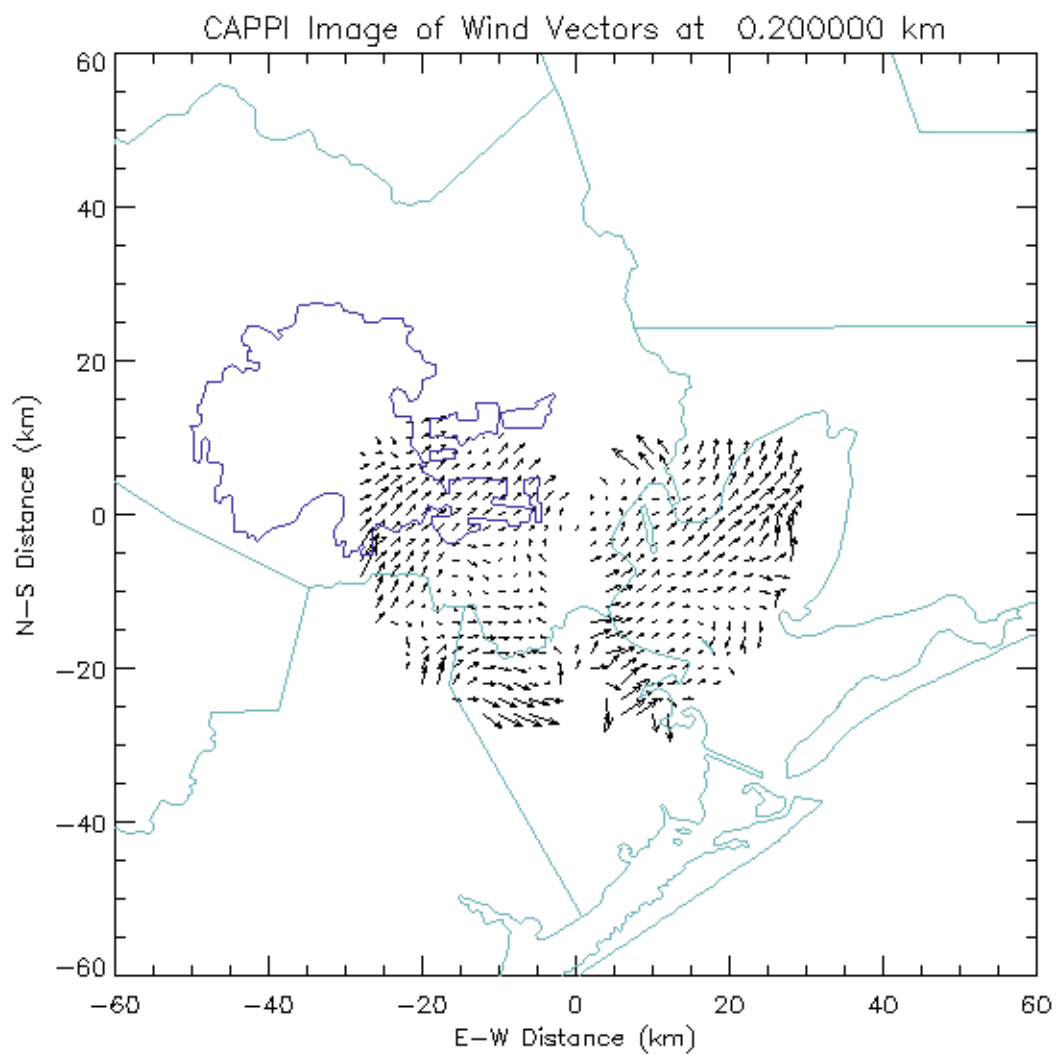


Figure 5: Dual-Doppler derived wind field at a height of 200 m using 3 km horizontal radii of influence and 200 m vertical radius of influence, 1536Z 10 August 2005.

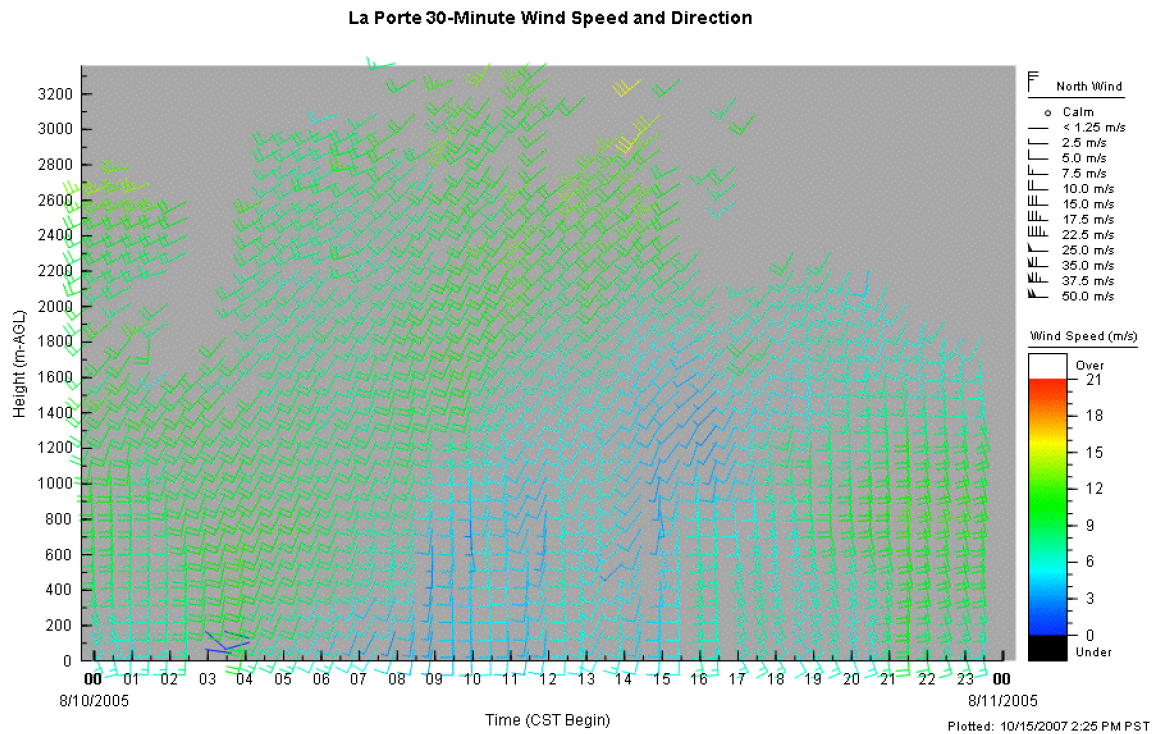


Figure 6: Wind speed and direction from the TCEQ radar wind profiler at La Porte, 10 August 2005 (courtesy of STI).

Problems were observed regarding the accuracy of the derived wind fields as compared to actual surface wind measurements. To illustrate the specific characteristics of the issues encountered, the case of 10 August 2005 will be presented.

On the morning of 10 August 2005, the TCEQ radar wind profiler in La Porte recorded uniform winds out of the south and southwest at 5-10 m/s extending from the surface to well above 1 km (Figure 6). The dual-Doppler derived wind field for an altitude of 200 m at 1200 – 1300 UTC on this day was chosen for analysis, and was expected to reflect

this actual wind field with a simple and uniform field of southerly and southwesterly wind vectors. Any convergence or divergence features were expected to appear either randomly (i.e. not linked to the geometry of the arrangement of the two radars) or associated spatially and temporally with a meteorological phenomenon such as the land-sea breeze circulation. Also, any peculiar features staying stationary with time and/or occurring along the baseline between the two radars were immediately deemed suspicious.

Figure 7 shows the dual-Doppler derived wind field from the SR1 and KHGX radars for 1201 UTC, 10 August 2005. Four areas of suspicion are labeled. These suspicious features were consistently present in derived wind fields. While these features hurt the feasibility of this data to be assimilated into mesoscale models, it is noteworthy that, for the most part, data in regions within the middle of the radar lobes and not geometrically significant to the radar configuration do reasonably well in reflecting the actual wind field.

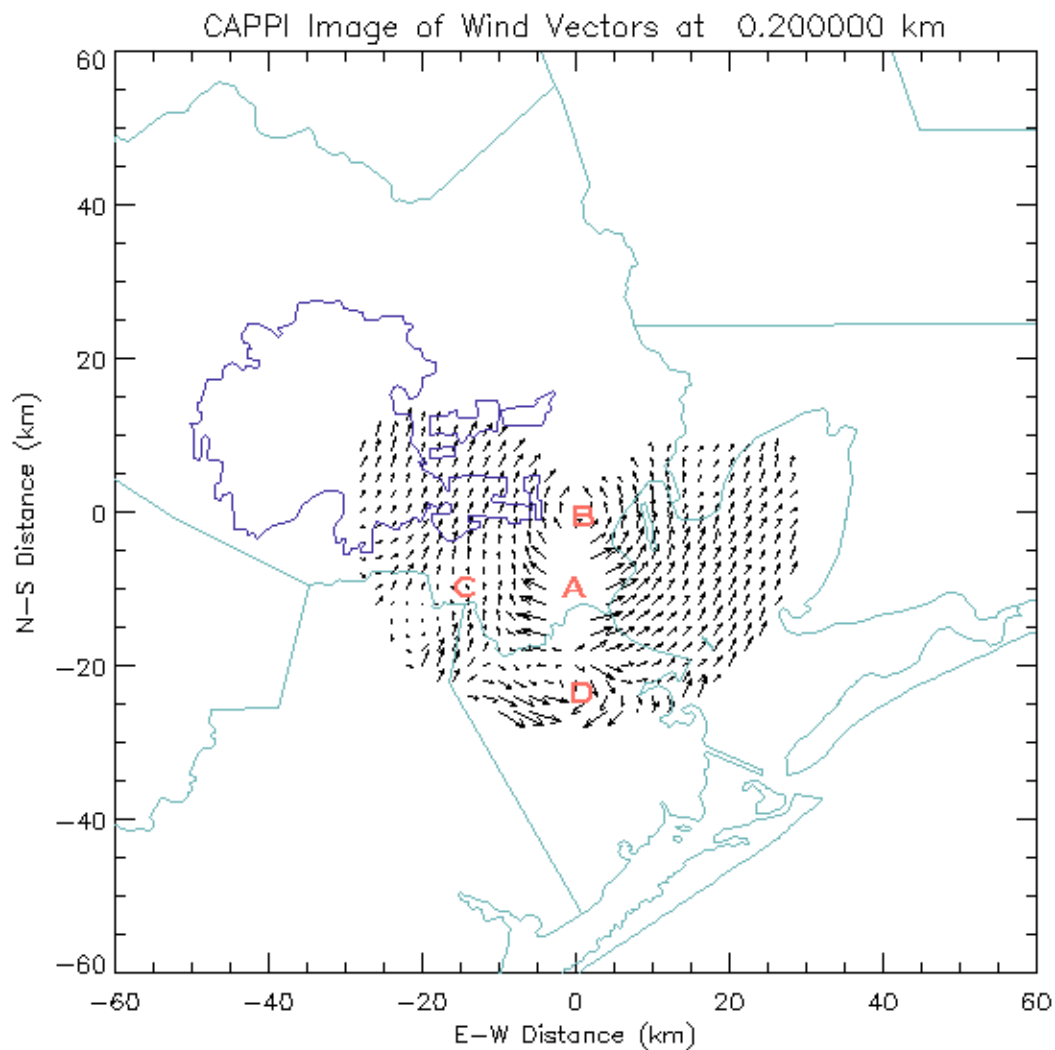


Figure 7: Dual-Doppler derived wind field for 1201 UTC, 10 August, 2005, with suspicious features labeled.

“A” refers to the strong divergence feature present along the baseline between SR1 and KHGX. Given the geometric significance of the location of this feature to the locations of the two radars, and the lack of meteorological phenomena that could be attributed to

such a wind pattern, this feature has to be considered erroneous. Another obvious area of suspicion is feature “B,” the strong tangential bias of the winds to the location of SR1. Again, this wind pattern is in a very geometrically significant area and cannot be associated with any kind of meteorological feature, thus it must be considered erroneous as well. These two features can almost be considered one larger, circular feature, and is likely evidence that SR1 is underestimating wind speeds, resulting in the skewing the direction of the derived wind vectors away from the radial direction of the underestimating radar compared to the actual wind direction.

Feature “C” is a region of weak derived wind speeds that stretches southwest to northeast across the western dual-Doppler lobe. This feature remains stationary and consistent in size and shape with time, and is not attributable to any kind of meteorological phenomenon. It also shows up well on the raw velocity data from SR1 as well. This is also erroneous data, and is likely a result of ground clutter or some other type of interference the SR1 radar experienced.

Finally, feature “D” is a noisy region south of the KHGX radar. Wind directions are fairly chaotic with time in this region, but consistently noisy and random, in the same location, and never associated with any kind of meteorological feature. There could be numerous reasons for this erroneous data. At times, this feature exhibited a hint of a circular pattern around the location of the KHGX radar, and thus could be another result of underestimation of winds. The proximity of this feature to the edge of the dual-

Doppler domain could also be the reason for the noisiness, as the edges of radar lobes tend to be the most susceptible to noisy returns.

The dual-Doppler derived wind field for a bit later in the day (1536 UTC) is shown in figure 8. The same four suspicious features are present in the same locations at this time as they were in the derived wind field at 1201 UTC. The divergence along the baseline is present, though the magnitudes of the erroneous winds are less than in the 1201 wind field. A tangential bias around the location of SR1 is present as well. The diagonal strip of weak returns on the western lobe, though a bit harder to make out, is still present, and the erratic wind signature south of KHGX is evident, and appears much noisier than in the 1201 UTC field. These four features are also present in the derived wind field two days later at 1512 UTC 12 August 2005 (Figure 9). These features, in fact, remained persistent in all of the dual-Doppler derived wind fields that were analyzed.

In some isolated areas (namely the regions denoted by A, B, C, and D in Figure 7), vector differences between the dual-Doppler derived winds and the actual measured winds were observed to be from ~ 5.0 m/s upwards to ~ 20.0 m/s. In the regions of the analyzed area that were not characterized by any suspicious features, vector differences were generally observed to be in the 1.0-2.0 m/s range. These vector differences can be compared to the RMS errors of 1.5 to 2.0 m/s cited by Nielsen-Gammon et al (2007) to be present in mesoscale models in the absence of dual-Doppler wind data.

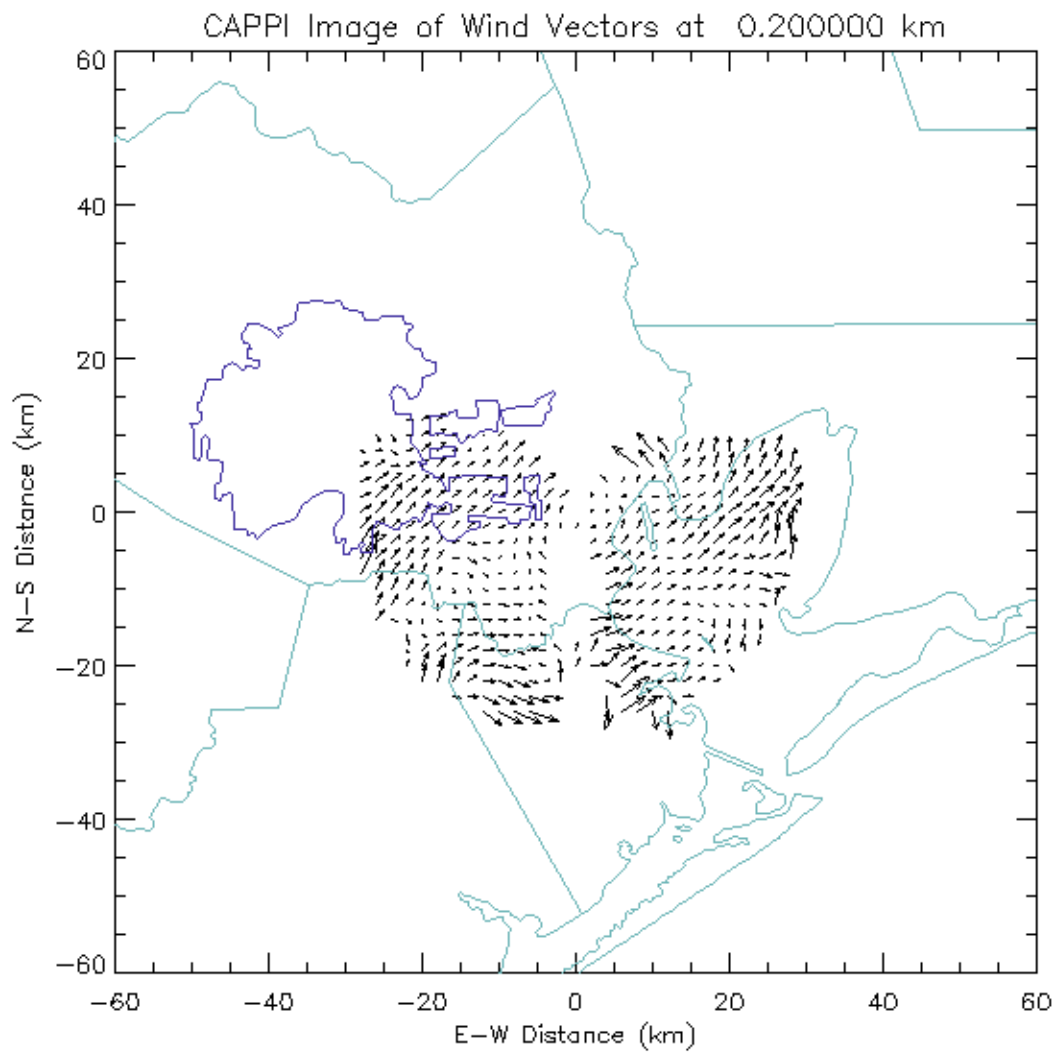


Figure 8: Dual-Doppler derived wind field for 1536 UTC, 10 August, 2005.

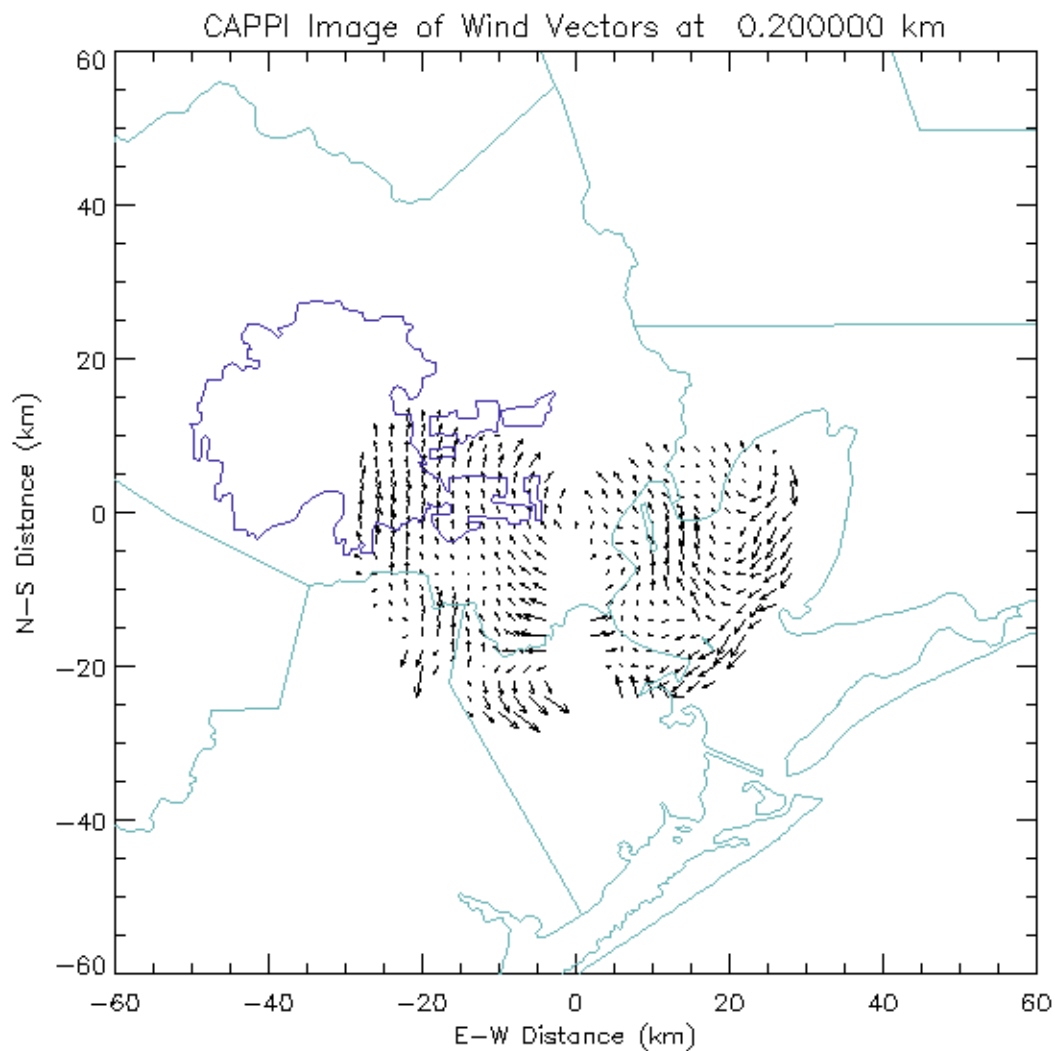


Figure 9: Dual-Doppler derived wind field for 1512 UTC, 12 August 2005.

6. Conclusions

In order to determine an ideal set of parameters for producing a dual-Doppler derived wind field from the data collected by SR1 and KHGX during the summer of 2005,

experimentation was done with values for beam-crossing angle and sphere of influence for each data point. It was determined that utilizing a minimum beam-crossing angle of 30°, setting the horizontal radii of influence in the x and y direction at 3 km, and setting the vertical radius of influence at 200 m resulted in a satisfactory wind field that was representative of the region while maintaining adequate data resolution.

In plotting the dual-Doppler derived wind field for a day in which winds were relatively uniform with time across the region, numerous erroneous features were consistently present, likely due to shortcomings in wind speed estimation by SR1 and/or ground clutter or other types of interference. Due to the consistent presence of these features and the magnitudes of the error associated with these features, it is likely not feasible to assimilate the dual-Doppler derived wind fields from SR1 and KHGX during TexAQS-II into mesoscale models to improve simulation accuracy. However, given that the error likely lies with SR1 and not KHGX, wind data from KHGX could be useful.

Data from SR1 may still be useful for case study analysis and model verification. The SR1 radar was stationed near the northwest corner of Galveston Bay and the entrance to the Houston Ship Channel. The development and progression of the Galveston Bay breeze, on days with a prominent Bay breeze front, will be detectable in the SR1 radar data as a linear enhancement to the reflectivity field combined with a horizontal discontinuity of radial velocity. The simultaneous detection of this feature in both reflectivity and velocity eliminates the errors that might have led to errors in the dual-Doppler reconstructions.

References

- Carey, L.D., V.A. McNear, J. Guynes, J.W. Nielsen-Gammon, F. Zhang., 2005:
Observations of Boundary Layer Winds over Houston and Dallas-Fort
Worth in Support of TexAQS II. Presented at TexAQS-II Field Intensive
Study Meeting. Available at
[http://www.tceq.state.tx.us/assets/public/implementation/air/am/workshop/
20060418/Carey-TAMU_C-Band_Radars.pdf](http://www.tceq.state.tx.us/assets/public/implementation/air/am/workshop/20060418/Carey-TAMU_C-Band_Radars.pdf)
- Gauthreaux Jr., S.A., D.S. Mizrahi, and C.G. Belser, 1998: Bird migration and bias of
WSR-88D wind estimates. *Wea. Forecasting*, **13**, 465-481.
- McNear, V.A., 2007: Low-level convergence and its role in convective intensity and
Frequency over the Houston lightning and rainfall anomaly. M.S. Thesis, Dept.
of Atmospheric Sciences, Texas A&M University, 190 pp.
- Oye, D. and M. Case, 1995: REORDER: a program for gridding radar data. Installation
and use manual for the Unix version. Boulder, CO, NCAR Atmospheric
Technology Division.
- Wilson, J.W., T.M. Weckwerth, J. Vivekanandan, R.M. Wakimoto, and R.W. Russel,
1994: Boundary layer clear-air radar echoes: origin of echoes and accuracy of

derived winds. *J. Atmos. Oceanic Technol.*, **11**, 1184-1206.